Use of SBS for forming diffraction-limited divergence and increasing the contrast of radiation in an excimer-laser system

N.G. Ivanov, V.F. Losev, and Yu.N. Panchenko

Institute of High-Current Electronics,
Siberian Branch of the Russian Academy of Sciences, Tomsk

Received February 1, 2001

The feasibility of using SBS to form diffraction-limited divergence and increase the contrast of radiation in a laser system based on electric-discharge XeCl amplifiers is studied experimentally. It is shown that the phase conjugation at SBS allows correcting for phase distortions in an active medium, as well as astigmatic and spherical aberrations in the optical channel, whereas the SBS itself allows obtaining the radiation contrast up to 10^6–10^7 as high.

Introduction

Excimer lasers are now the most efficient and powerful sources of coherent radiation in the UV spectral region. However, the high gain factor of their active media (g_0 = 0.05–0.15 cm^{-1}) and unstable or weakly coupled lower term of the lasing transition lead to low coherence of laser radiation. At the same time, many applications of excimer lasers require not only the high power, but also the high quality of radiation. To improve the quality of radiation in excimer lasers, various methods can be used.

One of the main methods to obtain a high-power pulse with low divergence and narrow line is amplification of a master-oscillator beam in a laser system. However, obtaining diffraction-limited divergence in such a system is usually complicated because of the presence of optical inhomogeneities in the amplifier active medium and in the atmospheric optical path, as well as optical aberrations. Under conditions that optical inhomogeneities in the laser system can hardly be eliminated, the method of phase conjugation (PHC) can be used to increase the spatial coherence of laser radiation. It is known that this method allows successful correction for the phase distortions of the wave front.[1,2]

Up to now the excimer laser systems with PHC were studied only for the case of a short pulse (no longer than 20 ns). In this case, the phase conjugation is achieved by use of stimulated Brillouin scattering (SBS).[1–4] Undoubtedly, it is interesting to study the feasibility of using PHC to improve the radiation divergence in laser systems with longer pulses, because the increase of pulse duration increases the output energy.

In interaction of laser radiation with matter, a high-contrast (high power ratio of the directed radiation and the noise component) beam is needed very often. For some applications (for example, in laser nuclear fusion[5] etc.) the contrast γ as high as $10^6 - 10^8$ is needed. The value of γ decreases in the presence of a residual noise component in the master-oscillator (MO) radiation, as well as due to appearance of double- and single-pass amplified spontaneous radiation (ASR) in the amplifying cascades. To increase the contrast in Nd lasers, a nonlinear medium based on SBS was earlier used.[6,7] In excimer lasers, no attempts to increase the contrast due to SBS have been undertaken until so far.

There are only a few papers in the literature on the influence of the laser optical path itself (optical elements, air) on the divergence of the amplified beam, and the possibility of correcting for the wave front distortions by PHC was not studied.

In this paper, we study experimentally the possibility of using SBS to form diffraction-limited divergence and to increase the contrast in a laser system based on electric-discharge XeCl amplifiers.

Experimental technique and instrumentation

In the experiments, we used three electric-discharge XeCl lasers with different pump-pulse duration. The laser discharge gap was preionized from a "plasma sheet" playing the role of an electrode. The active volume of the lasers usually was $1.5 \times 3.5 \times 60$ cm^3. The lasers operated in the Ne:Xe:HCl mixture with the total pressure of 2–4 atm and could emit pulses with the energy of 100–300 mJ and duration of 15–200 ns at the power half-maximum.

One of the lasers served as the MO. The MO laser beam had nearly diffraction-limited divergence (for the diameter of 1.4 mm), the line width of 0.01 cm^{-1}, 95% degree of polarization, duration of 50 ns, and the energy of 1 mJ per pulse. Two other lasers served as amplifiers in various optical schemes.

To make a correction for wave front distortions of the amplified radiation, we used the PHC method with SBS. The radiation was focused by a lens into a cell filled with hexane (C_6H_{14}) or SF_6. To obtain high efficiency of SBS and to exclude thermal effects in a nonlinear medium, we chose the optimal input geometry and intensity of the pump beam.

0235-6880/01/05 404-07 $02.00

The temporal shape of the incident and scattered beams was measured by a FEK 22SPU photodiode with 6LOR and S8–14 oscilloscopes. The radiation energy was measured with an IMO–2N power and energy meter. The divergence was determined with a mirror wedge of an attenuator and calibrated diaphragms in the focal plane of a lens (focal length F = 10 m).

Experimental results and discussion

Influence of the active medium

The capabilities of compensating for wave front distortions in the amplifier active medium were studied using a XeCl laser with a 300-ns long discharge current pulse. The influence of optical inhomogeneities on radiation divergence was studied under conditions of maximum gain factor in the active medium. We used the mixture Ne:Xe:HCl = 1400:10:1 at the pressure P = 4 atm and charging voltage U = 30 kV. The gain factor for a weak signal at the peak pumping current was $g_0 = 0.05$ cm^{-1}. It should be noted that this value remained almost unchanged during the pulse both in time and over the volume. The optical layout of this experiment is shown in Fig. 1*a*. The probing 15-ns long pulse with the energy of 25 mJ was formed in the first two lasers and injected into the long-pulse amplifier.

Figure 2 shows the distribution of the intensity I of the amplified radiation in the near and far zones at different moments of the discharge glow.

As is seen from Fig. 2, within 80 ns of the discharge glow, the divergence in the direction across the current started to worsen. From the intensity distribution in the near zone, it is seen that starting from the time of 100 ns, the width of the discharge decreased and by 195 ns the amplification existed only in two narrow zones. As this occurred, several stages were observed in the discharge glow.

At the first stage by the time of 80–100 ns, a homogeneous discharge with the mean current density ~ 350 A/cm^2 was observed. At the next stage, the discharge narrowed to the zone with the high strength of the electric field, in which the mean current density increased up to 700–800 A/cm^2. As this took place, macroinhomogeneities in the form of numerous channels with the cross dimension of 1 to 2 mm arose from anode and cathode plasma spots in the central zone. These channels were aligned in a row over the gap length with the density n = 6–8 cm^{-1} (the time of 120 ns) and glowed simultaneously with the volume discharge.

By the time of 170 ns, a zone, in which the passing beam did not experience amplification, arose on the anode side in the area of the diffuse volume discharge. This zone spread to the cathode, and 25–30 ns later the volume discharge transformed into a discharge with a thread-like structure, which can be discerned when recording the radiation on a more sensitive photographic material. In this case, formation of plasma spots was not observed on the anode.

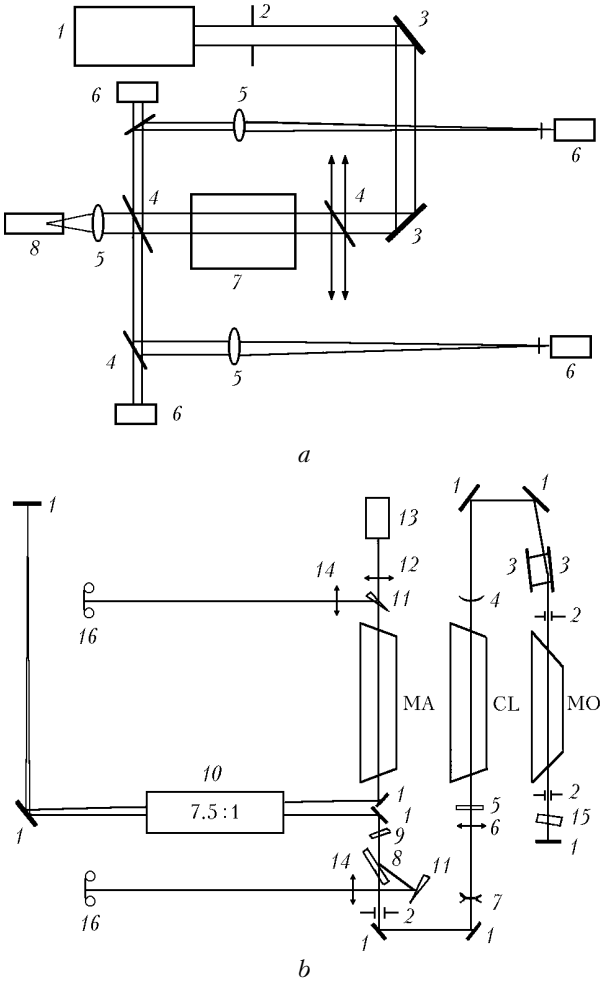

Fig. 1. Optical arrangement of the experiment: upper panel: laser system *1*, diaphragm ∅ = 0.01 m *2*, aluminum mirror *3*, quartz plate *4*, positive lenses with F = 6 and 10 m *5*; recording instrumentation (FEK 22SPU, IMO–2N) *6*, active medium of XeCl laser *7*, and cell with heptane *8*; lower panel: totally reflecting mirror *1*, diaphragm *2*, diffraction grating *3*, convex mirror with F = 6.34 m *4*; mirror with variable reflection coefficient *5*, lens with F = 0.5 m *6*, lens with F = 0.2 m *7*, polarizer *8*, λ/4 plate *9*, telescope *10*, wedge *11*, lens with F = (0.5, 1, 2) m *12*, cell with SF_6 *13*, lens with F = 3 m *14*, Fabry–Perot etalon *15*, photographic film *16*, main amplifier (MA), controllable laser (CL).

By the time of 195 ns, the properties of the active medium changed in the area of the volume discharge: it transformed from amplifying to absorbing ($g_0/\alpha < 1$) with the absorption coefficient $\alpha = 0.01$ cm^{-1} at the wavelength λ = 308 nm. This property of the medium then remained until termination of the first period of the current. This may be caused by the transformation of the volume discharge into the thread-like channels and fast burning-out of halogen in them due to the high current density.[8,9] As a result, the gain factor in this area decreased sharply, while the absorption coefficient increased and remained at the high level. At the same time, in the zone with a large number of macrochannels aligned along the length of the discharge gap, the input

signal continued to become stronger by the time of 195 ns, and the g_0/α ratio remained larger than unity during the whole discharge pulse.

It should be noted that in the case of formation of few macrochannels in the discharge $n < 1$ cm^{-1} (at inhomogeneous glow of the plasma sheet), the current traversing the gap contracted to these channels, and amplification in this zone terminated much faster. As to the zone, in which the discharge glow terminated completely, it did not affect markedly the intensity and divergence of the beam passing through it until termination of the first period of the current.

The observed increase in the divergence of the amplified radiation after the time of 80 ns could be connected both with the amplitude and phase inhomogeneity. The phase changes at macroinhomogeneities mostly due to different electron density n_e in the plasma, and this change at the length ∂z can be estimated by the equation[10]

$$(\partial\varphi/\partial z)_e = -\pi n_e/\lambda n_{cr}, \qquad (1)$$

where the critical electron density $n_{cr} = 1.17 \cdot 10^{22}$ cm^{-3}. Since in our case the macrochannels had a periodic structure along the electrodes, the phase change for the difference in the electron density in the volume discharge and the channel $\Delta n_e \sim 10^{15}$ cm^{-3} at the length $L = 0.6$ m is $\Delta\varphi = 0.25\lambda$. This change can lead to slight distortions of the wave front and insignificant decrease in the divergence of the amplified radiation.

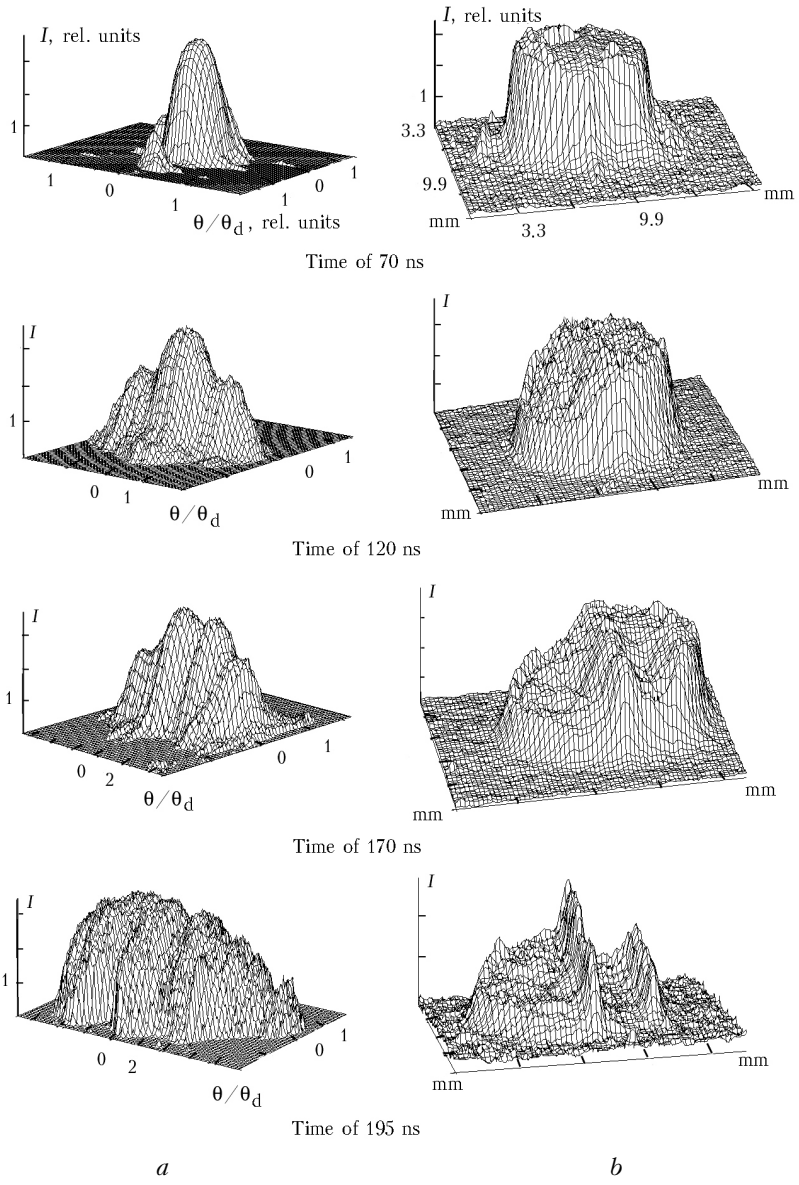

Fig. 2. Intensity distribution in the far (*a*) and near (*b*) zones at different time moments; θ is the radiation divergence, θ_d is the diffraction angle.

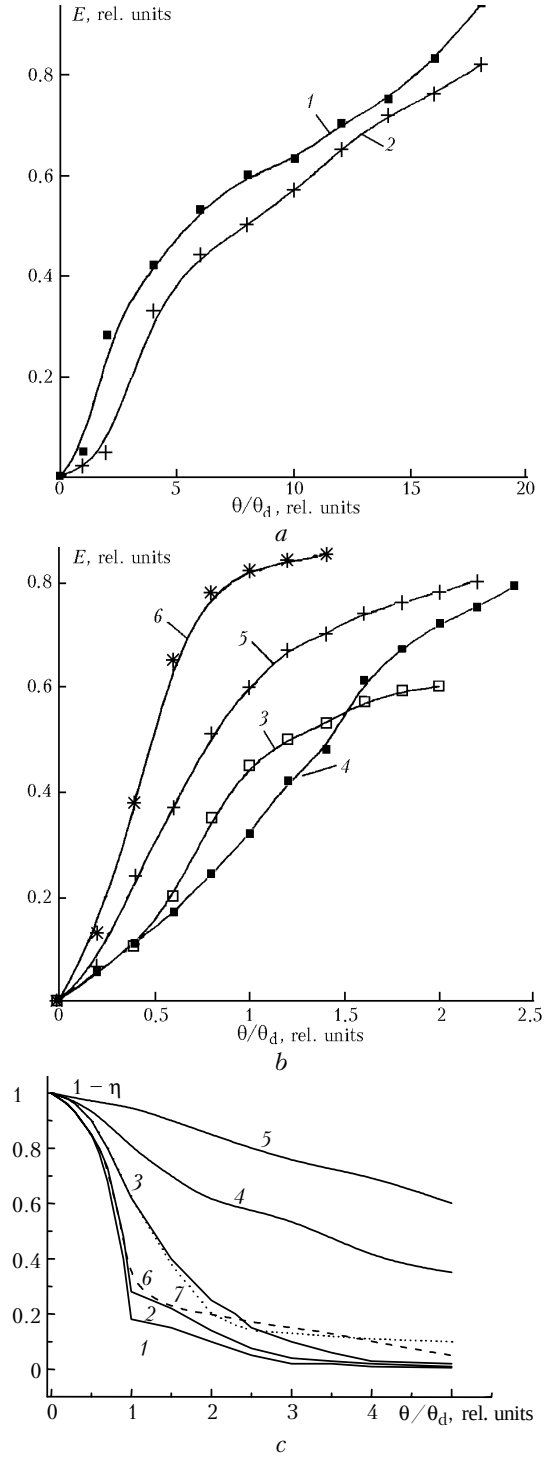

Fig. 3. Energy directional patterns: upper panel: for radiation incident on a nonlinear medium with the beam diameter of 75 (*1*) and 150 mm (*2*); central panel: initial radiation (*3*) and backward radiation (*4–6*), the curve *5* was obtained when heating a part of the optical path; lower panel: for the input (*1*), amplified (*2–5*) and reverse (*6*, *7*) beams at the time of 70 (*2*), 120 (*3*), 170 (*4*), 195 (*5*), 70 (*6*), and 120 ns (*7*); η is a fraction of the total radiation energy contained in the corresponding angle θ; θ_d is the diffraction angle (in the case of homogeneous distribution of radiation); *E* is the radiation energy.

Estimation of the phase change at microchannels (100–1000 channels per the active length) 200 μm in size with $n_e = 10^{17}$ cm^{-3} (Ref. 8) gives $\Delta\varphi = (0.4 - 4)\lambda$. This phase change can affect significantly the radiation divergence. Thermal and shock waves arising at gas-dynamics expansion of these microchannels can make an additional contribution to the change of the refractive index.[11] In our case, this manifests itself after 300 ns.

The effect of amplitude distortions on worsening of the directional pattern of the amplified beam was determined by the sharp change of amplification in the active medium along the beam cross section due to current redistribution. We can separate out two moments in time, 120 and 195 ns, in the evolution of the discharge width. At the first stage, the divergence of the amplified radiation did not change. At the second stage, the divergence increased roughly twice. At the third stage, when the cross size of the active medium was roughly 1–2 mm, the beam divergence increased roughly 10 times.

The results of studying the divergence of the amplified beam with the use of PHC at different moments of discharge glow are illustrated in Fig. 3*c*. As is seen from the figure, the directional patterns of the reflected beams obtained at 70 and 120 ns are close in the behavior to the directional patterns of the incident beams at the corresponding moments. The reflected beam carried ~70% energy of the pump beam. A part of this energy (~20%) corresponded to the component that did not experience phase conjugation and had a wide directional pattern. The cause for its appearance was, most likely, the noise properties of the SBS process. For the period of 170–190 ns, amplitude distortions increased considerably. Therefore, in this case, the signal reflected and re-passed through the amplifier did not reconstruct the wave front of the initial beam.

Influence of the optical path

The behavior of the divergence of the MO beam upon it passed the optical path of the laser system was studied in the optical arrangement shown in Fig. 1*b*. In this case, the directional pattern of the diffraction-limited beam could be affected by both inhomogeneities of the refractive index in the atmospheric air and aberration arising as the beam passed through optical elements of the system.

In our experiment, the radiation leaving the laser system (LS) was collimated by lenses *6* and *7* and, having passed through the beam-splitting quartz plate *8*, was then expanded by the telescope *10* with the magnification $M = 7.5$. The length of the path passed by the expanded beam varied from 0.2 to 24 m for different experimental conditions. Coming back at a small angle to the opposing beam, the laser beam again contracted to the diameter ~ 20 mm and was focused into the cell filled with SF_6 by the lens *12* with $F = 1$ m. The radiation was recorded by dividing a part of the light flux by the quartz plates installed before

and after the telescope, as well as in front of the lens *12*.

The measured results on the angular distribution of radiation in the far zone for the radiation incident on the nonlinear medium and the returned radiation are shown in Figs. 3*a* and *b*. Somewhat higher divergence of the beam 150 mm in diameter was caused mostly by air turbulence. As this took place, the focal spot broke into separate chaotically arranged spots. In the case of increase of the turbulent flows in the transportation channel of the beam 75 mm in diameter (with a point-like thermal source situated after the telescope), the structure of its focal spot became analogous to that for the beam 150 mm in diameter (without thermal source).

Recording of focal spots for the beams (with different diameters) reflected from the nonlinear medium and re-passed the optical path showed that the degree of compensation for distortions is different for beam of different diameters. It can be estimated quantitatively from the measured energy distributions of this radiation shown in Figs. 3*a* and *b*. At the beam diameter of 75 mm, the reversed radiation has the diffraction-limited divergence, i.e., the divergence somewhat lower than that of the incident beam. This may be caused by the threshold effect of the SBS (Fig. 4*a*, row *3*).

In the case of increasing wave front distortions for the 75-mm beam, the higher quality of the PHC pumping was observed; the reflected signal in the far zone had similar structure of the intensity, and it contained 60% energy within the diffraction angle.

Worsening of the PHC quality for the 150-mm beam may be caused by the presence of aberration effects at optical elements of the telescope. In this connection, to separate the wave front distortions, the beam acquired in the air and on optical elements, we conducted the experiments to study the possibility of making the phase conjugation of a beam experienced distortions due to astigmatic and spherical aberrations of different degree, as well as in the case that the beam passes through air sections having a sharp gradient of the refractive index over the cross section.

The optical arrangement of these experiments is shown in Fig. 1*a*. The output laser beam 13 mm in diameter had the diffraction-limited divergence (Fig. 4*a*, row *1*). To introduce astigmatic distortions in the wave front of the pump beam, the lens focusing the laser radiation into the cell with the nonlinear medium was set an angle of 9° 47′ to the optical axis. Figure 4*a* (row *2*) shows the intensity distribution of the radiation in the far zone after passage through the lens and after PHC compensation for distortions.

Measurement of the directional pattern of the scattered radiation showed that the quality of the PHC worsens, as the energy of the pump beam increases. In this case, "wings" containing the major part of energy arise from the central lobe of the directional pattern in parallel to the direction of the first waist. This effect can be presumably explained by the presence of the noise component with a wide directional pattern determined by the profile of the caustic surface of the astigmatic beam, as well as by screening of a part of the incident radiation by the first focus because of the presence of two spaced apart focal waists along the beam path. If one of the focuses was outside the scattering volume, the beam PHC was completely absent; the divergence of the backscattered radiation had a wide angular component in the direction normal to the rest waist.

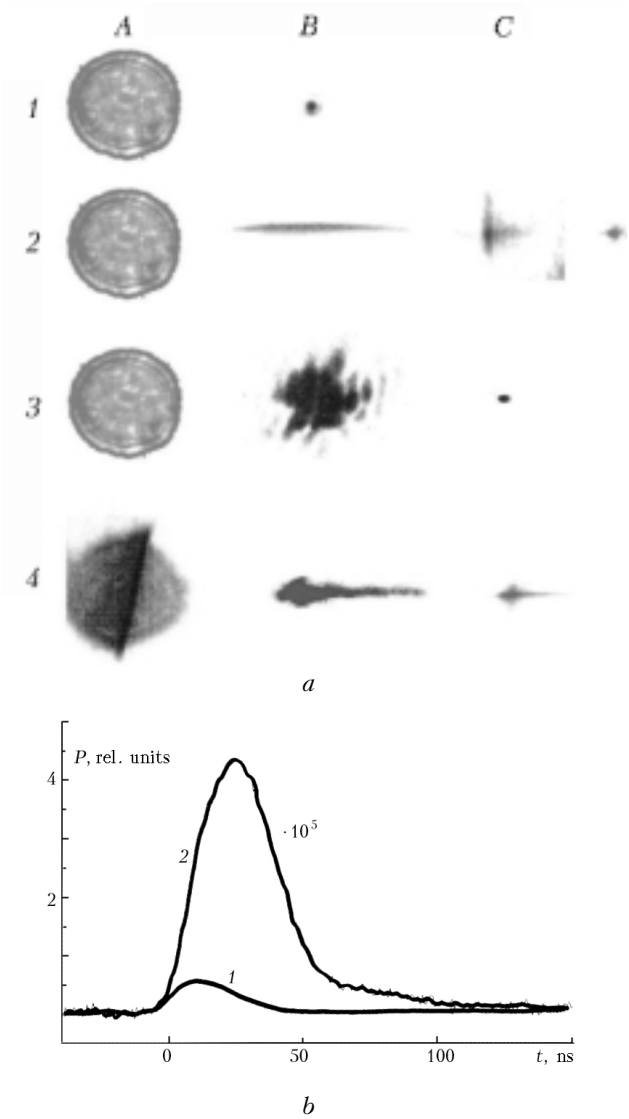

Fig. 4. Distribution of radiation power P in the near (A) and far (B, C) zones after distortion (B) and correction (C) of the wave front due to PHC (a) and the time behavior of the amplified (*2*) and noise (*1*) components (b); upper panel: pump beam *1*, lens astigmatism *2*, air turbulence (L = 15 m, beam diameter of 75 mm) *3*, narrow thermal air flow *4*; ($2 - C$) – beam energy of 30 (left) and 10 mJ.

Spherical aberrations of the wave front on the lens telescope increased the divergence of the incident beam.

The energy directional pattern of this beam was measured in the plane of the best focusing, where the size of the focal spot was minimum. In this case, the diameter of the focal spot can be estimated from the equation[12]

$$D = F\theta_d + Rd^3/32F^2, \quad (2)$$

where θ_d is the diffraction-limited divergence of the beam; $R = 1/(1 - 1/n)^2\,[(2/n + 1)\,\alpha^2 - (2 + 1/n)\times \times \alpha + 1]$ is the aberration parameter of the lens. For a thin lens $\alpha = 1/n(1 - r_1/r_2)$, where r_1 and r_2 are the curvature lengths of respectively the first and the second surfaces of the lens; n is the refractive index.

This type of distortions was compensated for in the backward passage of the beam reflected from the nonlinear medium. Nevertheless, it should be noted that the quality of PHC depended on the intensity of the pump radiation. At the low pump power close to the SBS threshold, some spatial-angular filtering of the pumping beam occurred.

Increasing the gradient of the refractive index in the beam cross section, we tried to determine the boundary conditions for wave front distortions, at which the PHC effect is still possible. For this purpose, using an extended thermal source arranged in parallel with the optical axis, we modeled a narrow laminar thermal flow spreading across the laser beam. In this case, a part of the wave front acquired considerable distortions, which led to the change in the shape and the intensity profile of the beam in both far and near zones (Fig. 4*a*, row *4*). It is seen that the wave front distortions in this case are partially compensated for.

Improvement of the radiation contrast

The radiation contrast was studied after the double-pass amplification of the MO beam in a short-pulse amplifier with $g_0 = 0.16$ cm^{-1} immediately at its exit and at the distance of 3 m from the exit window. The results obtained at the reflection from an aluminum mirror and from the SBS medium were compared.

The high gain factor of the active medium allowed spontaneous radiative fluxes propagating at large angles to the optical axis to be amplified significantly. At the exit from the double-pass amplifier, the angular spectrum of the directivity of spontaneous noise consisted of two components given by the double-pass and single-pass ASR. In the first case the angular directivity ranged up to 5 mrad, in the second case it ranged from 20 mrad and higher. In the absence of the input signal, the energy ratio of these fluxes was 50/1. If a signal entered from the side of the amplifier window, the fraction of the spontaneous noise changed depending on the radiation power entered into the active medium. Two limiting cases were considered: nearly linear regime (input signal with the power ~ 100 W) and amplification in the regime of saturation. The conditions, under which amplification of a weak signal was studied, took place in the case of using the MO beam with the typical output energy of 5–10 μJ. The second regime takes place in the case of high input energy fluxes; in our case, the maximum power density of radiation injected into the amplifier achieved 10 kW/cm^2. The measured part of ASR in the laser beam after its double-pass amplification with the use of the aluminum mirror (for the input signal with the power density of 50 W/cm^2) was 60%, and for 10 kW/cm^2 it was 35% at the total output energy of the amplified beam of 15 and 70 mJ, respectively.

The use of SBS as a nonlinear filter allows the ASR component to be filtered out rather efficiently. If the threshold gain increment G is equal to 25, then the threshold pump power

$$P_0 = 25S/gL, \quad (3)$$

where S (the cross section of the scattering area) = $= \pi d^2/4 = \pi F^2\alpha^2/4 \sim F^2\alpha^2$; L is the length of the interaction zone; g is the SBS gain factor. It is seen that the threshold SBS power increases as a square function of the divergence of the pump radiation. This factor leads to a significant difference between the threshold values for the laser beam and the ASR flux. In our case, this ratio ranged from 10^3 to 10^4. This allowed the contrast of the amplified radiation to be improved up to $\gamma = 420$.

However, in addition to the amplifier noise, the output radiation includes a broadband ASR with the angular directivity of 10^{-4} because of the presence of background in the MO beam to be amplified. In our case in the MO beam with the peak power of 25 kW and the spectral width of 0.01 cm^{-1}, the radiation contrast (power ratio of ASR at the filtered-out transition 0–1 to the laser radiation at the working transition 0–2) was no worse than 420. When changing conditions of the radiation formation in MO, due to a decrease in the gain factor of the active medium and energy deposition into the discharge from the peaking capacitor, the contrast of the output radiation decreased down to 45 and 300 at the leading and trailing parts of the pulse, respectively. This effect was caused by slower formation of narrow-band radiation because of the increase of nonselective loss in the cavity. Since the divergence of ASR in the MO beam exceeds the divergence of the narrow-band beam by no more than two to three times, the radiation was selected by the width of the spectral line. In this case, the scattering can be considered with both spatially coherent and incoherent radiation.

In the former case, the conditions characteristic of scattering of monochromatic radiation are considered, i.e., the interaction length is shorter than the coherence length of this radiation. In this approximation, the SBS efficiency is independent of the spectral width of the pump radiation $\Delta\nu$, and amplification follows the e^G law, at $I > I_{cr} = 4\pi\Delta\nu/g$. In the case of incoherent radiation, the SBS efficiency drops sharply. The amplification at a broadband pump is estimated in Ref. 13. According to this estimate

$$G = \frac{L}{2}\{gI - 8\Delta\nu - 8\Delta\nu_0 +$$

$$+ [(gI - 8\Delta\nu - 8\Delta\nu_0)^2 + 32\Delta\nu_0\, gI]^{0.5}\}, \quad (4)$$

where $\Delta\nu_0$ is the width of the spontaneous Brillouin line.

Form Eqs. (3) and (4) we have

$$P/P_0 = 1 + \Delta\nu\, L/3, \quad (5)$$

where P is the pump power; P_0 is the threshold pump power at $\Delta\nu < \Delta\nu_0$. In the experiments, we determined the conditions, under which the contrast of the amplified radiation is improved up to $\gamma = 10^5$ (Fig. 4*b*). The increase of the contrast of the MO radiation from 4 up to 10^6 was observed at the incident beam energy no higher than 20 mJ. As the energy of the pump beam increased, the contrast in the amplified beam kept constant. To achieve the high contrast of the amplified radiation with the contrast of the input MO beam $\gamma = 50$, the energy of the pump radiation had to be decreased down to 10 mJ.

Conclusions

1. If various inhomogeneities are present in the active medium of the XeCl laser, the beam divergence is largely affected by redistribution of the gain factor profile. As macroinhomogeneities develop, some parts of the laser beam are amplified, and in the case of microinhomogeneities some parts of the laser beam are absorbed. The joint effect of all inhomogeneities existing in the laser medium led roughly to a 10 times increase of the divergence of the transmitted radiation. The use of PHC allows the diffraction-limited divergence of the amplified beam to be kept for 170 ns after the discharge initiation. In later time, this method was shown to be ineffective.

2. The XeCl laser beam with the initial divergence $\theta = 10^{-5}$ rad having passed the laboratory path $L \cong 15$ m changed the value of θ up to $1.5 \cdot 10^{-4}$ rad because of atmospheric turbulence. This type of wave front distortions can be corrected with PHC at SBS.

3. The PHC method allows the correction for astigmatic and spherical aberrations of the XeCl laser beam up to 10 θ_d.

4. With the use of SBS, the contrast of the XeCl laser radiation can be improved by up to 10^6–10^7.

References

1. M. Slatkin, I.J. Bigio, B.J. Feldman, and R.A. Fisher, Opt. Lett. **7**, No. 3, 108–110 (1982).
2. M.C. Gower and R.G. Caro, Opt. Lett. **7**, No. 4, 162–163 (1982).
3. Yu.F. Bychkov, V.F. Losev, and Yu.N. Panchenko, Kvant. Elektron. **19**, No. 7, 688–690 (1992).
4. I.J. Bigio, B.J. Feldman, R.A. Fisher, and M. Slatkin, IEEE J. Quantum. Electron. **17**, No. 12, 220–223 (1981).
5. G. Brederlov, E. Fill, V. Fuss, K. Hola, R. Folk, and K.I. Vitte, Kvant. Elektron. **3**, No. 4, 906–913 (1976).
6. S.B. Kormer, S.M. Kulikov, V.D. Nikolaev, A.V. Senik, and S.A. Sukharev, Pis'ma Zh. Teor. Fiz. **5**, No. 4, 213–216 (1979).
7. V.M. Gulevich, A.A. Ilyukhin, V.A. Maslyankin, and A.V. Shelobolin, Kvant. Elektron. **9**, No. 3, 537–541 (1982).
8. M.J. Kushner, IEEE Trans. Plasma Sci. **19**, No. 2, 387–391 (1991).
9. A.V. Dem'yanov, I.V. Kochetov, A.P. Napartovich, M. Capitelli, and S. Longo, Kvant. Elektron. **22**, No. 7, 673–682 (1995).
10. A.V. Dem'yanov, A.A. Deryugin, N.A. Dyatko, N.N. Elkin, I.V. Kochetov, A.P. Napartovich, and P.I. Svotin, Kvant. Elektron. **17**, No. 9, 1150–1155 (1990).
11. V.V. Borovkov, A.V. Andramanov, and S.L. Voronov, Kvant. Elektron. **26**, No. 1, 19–24 (1999).
12. A.G. Grigor'yants and I.N. Shiganov, *Laser Welding of Metals* (Vysshaya Shkola, Moscow, 1988), 100 pp.
13. V.I. Popovichev, V.V. Ragul'skii, and F.S. Faizullov, Pis'ma Zh. Eksp. Teor. Fiz. **19**, No. 6, 350–355 (1974).